JBC Papers in Press. Published on March 3, 2017 as Manuscript M116.762831
The latest version is at http://www.jbc.org/cgi/doi/10.1074/jbc.M116.762831

Identification of a feedback loop involving beta-glucosidase 2 and its product sphingosine sheds light on the molecular mechanisms in Gaucher disease

Sophie Schonauer[1], Heinz G. Körschen[2], Anke Penno[3], Andreas Rennhack[2], Bernadette Breiden[4], Konrad Sandhoff[4], Katharina Gutbrod[5], Peter Dörmann[5], Diana N. Raju[1], Per Haberkant[6], Mathias J. Gerl[7#], Britta Brügger[7], Hila Zigdon[8], Ayelet Vardi[8], Anthony H. Futerman[8], Christoph Thiele[3], Dagmar Wachten[1,9]

[1]Center of Advanced European Studies and Research (caesar), Minerva Max Planck Research Group, Molecular Physiology, Bonn, Germany
[2]Center of Advanced European Studies and Research (caesar), Department of Molecular Sensory Systems, Bonn, Germany
[3]LIMES Institute, Department of Cell Biology of Lipids, University of Bonn, Bonn, Germany
[4]LIMES Institute, c/o Kekulé-Institute, University of Bonn, Bonn, Germany
[5]Institute of Molecular Physiology and Biotechnology of Plants, University of Bonn, Bonn, Germany
[6]Proteomic Core Facility, EMBL Heidelberg, Heidelberg, Germany
[7]Biochemie-Zentrum (BZH), Ruprecht-Karls-University Heidelberg, Heidelberg, Germany
[8]Weizmann Institute of Science, Department of Biomolecular Sciences, Rehovot, Israel
[9]Institute of Innate Immunity, University Hospital, University of Bonn, Bonn, Germany
[#]current address: Lipotype GmbH, Tatzberg 47, 01307 Dresden

Running title: GBA2 in Gaucher disease

To whom correspondence should be addressed: PD Dr. Dagmar Wachten, Center of Advanced European Studies and Research (caesar), Ludwig-Erhard-Allee 2, 53175 Bonn, Germany; phone: +49-228-9656-311, fax: +49-228-9656-9311, email: dagmar.wachten@caesar.de

Keywords: GBA2, glucosylceramide, Gaucher disease, GBA1, glucocerebrosidase, sphingosine

ABSTRACT

The lysosomal acid beta-glucosidase GBA1 and the non-lysosomal beta-glucosidase GBA2 degrade glucosylceramide (GlcCer) to glucose and ceramide in different cellular compartments. Loss of GBA2 activity and the resulting accumulation of GlcCer results in male infertility, whereas mutations in the *GBA1* gene and loss of GBA1 activity cause the lipid-storage disorder Gaucher disease. However, the role of GBA2 in Gaucher disease pathology and its relationship to GBA1 is not well understood. Here, we report a GBA1-dependent down-regulation of GBA2 activity in patients with Gaucher disease. Using an experimental approach combining cell biology, biochemistry, and mass spectrometry, we show that sphingosine, the cytotoxic metabolite accumulating in Gaucher cells through the action of GBA2, directly binds to GBA2 and inhibits its activity. We propose a negative feed-back loop, in which sphingosine inhibits GBA2 activity in Gaucher cells, preventing further sphingosine accumulation and, thereby, cytotoxicity. Our findings add a new chapter to the understanding of the complex molecular mechanism underlying Gaucher disease and the regulation of beta-glucosidase activity in general.

Gaucher disease is one of the most common lysosomal storage disorders in humans. It results from a deficiency in the activity of the lysosomal enzyme, acid beta-glucosidase GBA1 (also termed GCase) (1). So far, more than 200 different mutations in the *GBA1* gene have been identified in Gaucher patients (2), all leading to the loss of enzyme activity, resulting in GlcCer accumulation in the lysosome. This is predominantly evident in tissue macrophages,

which turn into massively enlarged "Gaucher" cells, causing an up to 25-fold increase in organ size (organomegaly) of liver and spleen (3,4). Gaucher disease has been classified into three major subtypes, namely types I, II, and III (4). Type I is the most common, with patients displaying organomegaly of liver and spleen and defects in lung and bone marrow. Type II patients have the acute infantile neuronopathic form, characterized by severe neurological defects and an early onset of disease. These patients usually die within the first 2-3 years of life, whereas type III patients develop slowly progressive neuropathology. It has been assumed that residual GBA1 activity might help to predict the severity of Gaucher disease, but the severity of the disease even differs between patients carrying the same mutation (5). Thus, little genotype-phenotype correlation has been established so far.

How the accumulation of GlcCer in the lysosomes causes the complex Gaucher pathology is not well understood. Moreover, deficiency of GBA1 also causes accumulation of glucosylsphingosine (GlcSph) (6-8), which may also contribute to the neurological manifestation (9,10). It has been proposed that in Gaucher cells, both, GlcCer and GlcSph, leave the lysosome, becoming substrates for the non-lysosomal beta-glucosidase GBA2 (11,12), which resides at the cytoplasmic surface of the ER and *cis*-Golgi (13). In turn, GBA2 might hydrolyze GlcCer to glucose and ceramide and GlcSph to glucose and sphingosine (11,12). Ceramide can be further broken down to sphingosine and a fatty acid by neutral ceramidases. Hence, on the background of reduced GBA1 activity in lysosomes and leakage of its substrates outside the lysosomes, GBA2 activity might lead to an increased generation of sphingosine at the ER and *cis*-Golgi. It has been proposed that sphingosine is the cytotoxic metabolite that causes some of the defects associated with Gaucher disease, at least upon its chronic accumulation (12). In fact, deletion of GBA2 rescued some of the pathologies by reducing the accumulation of sphingosine (12). This is in line with our previous findings, indicating that GBA2 activity is altered when GBA1 activity is lost (13).

Here, we set out to investigate the role of GBA2 in Gaucher disease. We demonstrate that GBA2 activity depends on GBA1 activity, but not *vice versa*. GBA2 activity is inhibited by the cytotoxic metabolite sphingosine, which directly binds to GBA2. Our results suggest a negative feed-back loop in Gaucher cells, in which sphingosine prevents its excessive accumulation by inhibiting the activity of GBA2 through direct binding.

RESULTS

GBA2 activity is down-regulated in the absence of GBA1 activity - Based on our previous results (13), we analyzed GBA2 activity in fibroblasts from different types of Gaucher patients and in control fibroblasts using a fluorescence-based activity assay (13) that contains the artificial and water-soluble substrate 4-methylumbelliferyl-beta-D-glucopyranoside (4-MUG) and determines GBA1 activity at pH 4 and GBA2 activity at pH 6. For each pH, we included the GBA1-specific inhibitor conduritol B epoxide (CBE) and the GBA2-inhibitor *N*-butyldeoxynojirimycin (NB-DNJ) at concentrations that only inhibit the respective enzyme (13). As expected, GBA1 activity was almost absent in hypotonic lysates from Gaucher fibroblasts, with residual activities of 8%, 2.6%, and 5.6% for type I, II, and III, respectively (Fig. 1A). In line with our earlier findings (13), GBA2 activity in all types of Gaucher fibroblasts was decreased to around 60% of the activity in control cells (Fig. 1B). There was no difference in GBA2 activity between fibroblasts derived from patients with different genotypes and phenotypes, indicating that GBA2 activity is reduced independent of the Gaucher genotype and phenotype. To confirm this result, we measured GBA2 activity in two independent GBA1-deficient human fibroblast-like cell lines (HAP1) generated via CRISPR/Cas9 (Fig. 1C, D). The first GBA1-deficient HAP1 cell line (HZGHC002786c001, abbreviated #001) contains a 479 bp insertion in exon 6 of the *GBA1* gene and the second GBA1-deficient HAP1 cell line (HZGHC002786c010, abbreviated #010) contains a 1 bp insertion in exon 6, both resulting in a frame shift and, therefore, in gene silencing. In both cell lines, GBA1 activity was absent and GBA2 activity was reduced by ~40% (Fig. 1C, D). As a control, we determined the GBA1 activity in two independent GBA2-deficient human fibroblast-like cell lines generated via CRISPR/Cas9 (Fig. 1E, F). However, in the absence of GBA2 activity, GBA1 activity remained largely unchanged (Fig. 1E, F). In summary, GBA2 activity is down-regulated in the absence of GBA1 activity, but not *vice versa*.

To study whether the decrease in GBA2 activity is due to a change in GBA2 expression, we analyzed GBA2 mRNA and protein expression. The mRNA expression in dermal fibroblasts from different types of Gaucher and control patients

was determined using quantitative real-time PCR (Fig. 1G, H). For both, GBA1 and GBA2, there was no significant difference in relative mRNA expression between control fibroblasts and Gaucher fibroblasts from the different genetic backgrounds (Fig. 1G, H). Protein expression in dermal fibroblasts from Gaucher and control patients was analyzed by Western blot (Fig. 1I). The GBA1 protein level in fibroblasts from Gaucher patients was significantly reduced compared to control cells with GBA1 expression being lowest in fibroblasts from type II patients (Fig. 1J, K). However, GBA2 protein expression remained largely unchanged in control and Gaucher fibroblasts (Fig. 1J, K). Thus, down-regulation of GBA2 activity in the absence of GBA1 activity is not due to a decrease in GBA2 mRNA or protein expression.

GBA2 activity depends on GBA1 activity in vitro and in vivo - To gain mechanistic insight how GBA1 controls GBA2 activity, we analyzed whether blocking GBA1 activity is sufficient to reduce GBA2 activity. Here, we applied a pharmacologic approach. Control human fibroblasts were treated with 25 µM CBE for 48 h to block GBA1 activity (Fig. 2A, B). Of note, this CBE concentration does not block GBA2 activity (13). GBA1 activity was dramatically reduced in CBE-treated cell lysates compared to the non-treated controls (Fig. 2A). In line with our findings from Gaucher and GBA1-deficient fibroblasts, GBA2 activity in CBE-treated cells was reduced to ~39% of the activity in non-treated control cells (Fig. 2B). These results demonstrate that blocking GBA1 activity is sufficient to reduce GBA2 activity. We also tested this experimental paradigm in HEK293 cells transiently over-expressing mGBA2 and endogenously expressing GBA1 (Fig. 2C, D). Again, full block of GBA1 activity (Fig. 2C) reduced GBA2 activity to ~46% of the activity in non-treated control cells (Fig. 2D). As a control, we incubated embryonic fibroblasts from GBA1-deficient mice with 25 µM CBE for 48 h (Fig. 2E, F), which allows to measure CBE-dependent effects on GBA2 activity independent of a change in GBA1 activity. GBA1-deficient embryonic fibroblasts lack GBA1 activity (Fig. 2E), and the activity of GBA2 remained unchanged in these cells (Fig. 2F). In addition, we analyzed GBA2 protein expression in CBE-treated HEK293 cells over-expressing mGBA2, but there was no difference between treated and non-treated cells (Fig. 2G, H). We also performed the experiments *vice versa* in HEK293 cells over-expressing mGBA2 by blocking GBA2 activity with 2 µM NB-DNJ for 48 h (Fig. 2I, J). Whereas GBA2 activity was completely abolished in NB-DNJ-treated cells (Fig. 2J), GBA1 activity remained unchanged (Fig. 2I). Thus, our results suggest that GBA1 activity regulates GBA2 activity, but not *vice versa*, and that the regulation occurs independently of changes in protein expression.

Next, we analyzed the time course of the GBA1-dependent regulation of GBA2 activity. GBA1 activity was blocked with 25 µM CBE for 10 min up to 48 h (Fig. 2K). GBA1 activity was significantly reduced after three hours of CBE-treatment and was maximally blocked after 24 h (Fig. 2K). Interestingly, GBA2 activity was only reduced when GBA1 activity was almost absent (Fig. 2K). This result suggests that GBA2 activity responds to GBA1-dependent changes in the cell that take some time to develop, e.g. the accumulation of the substrates, GlcCer and GlcSph, in the lysosomes or the changes of downstream metabolites in the cytoplasm.

To investigate whether the GBA1-dependent regulation of GBA2 activity occurs not only in cell culture, but also in mice *in vivo*, we used the following approach. A Gaucher phenotype can be obtained by intra-peritoneal (i.p.) injection of low doses of CBE (14,15). Eight days old 6OlaHsd mice were injected with 25-100 mg CBE/kg/day for 10 days. After treatment, mice were sacrificed and the brain was dissected. GBA1 and GBA2 activities were assayed in hypotonic brain lysates from CBE-treated and control mice. All tested CBE concentrations blocked GBA1 activity by >85% (Fig. 3A) (15). In line with our earlier findings, GBA2 activity was also reduced at all CBE concentrations tested (Fig. 3B). Of note, at high concentrations, CBE also inhibits the activity of GBA2 (13,16). The final concentration of CBE in the brain is difficult to estimate. However, the reduction in GBA2 activity was similar, independent of the applied CBE dose (Fig. 3B), indicating that the reduction of GBA2 activity is GBA1-dependent and not due to a direct inhibition by CBE. As a control, we also analyzed GBA2 protein expression in CBE-treated mouse brains compared to controls (Fig. 3C, D). However, GBA2 protein expression was not affected by CBE treatment. Thus, the GBA1-dependent regulation of GBA2 activity occurs not only *in vitro* in isolated cells in culture, but also seems to be present *in vivo*, independent of changes in protein expression levels.

Investigating the underlying mechanism - Previous studies have reported an increase of GBA2 activity in cells from Gaucher patients (17,18). This is in contrast to our findings, which

is why we first performed additional experiments to verify our experimental set-up. Loss of GBA1 activity results in accumulation of GlcCer in the lysosome (2) and, thereby, in an increase in the amount of natural substrate for GBA2. Therefore, we determined the total amount of GlcCer in dermal fibroblasts from control and Gaucher patients by mass spectrometry (Fig.4A). Total GlcCer levels were not different between Gaucher fibroblasts and controls (Fig. 4A; control: 2.6 pmol/µg protein, type I: 3.0 pmol/µg protein, type II: 3.7 pmol/µg protein, type III: 3.6 pmol/µg protein), similar to what has been published before (19). In our assay, we use 75 µg of hypotonic lysates and 50 nmol 4-MUG per reaction, representing an at least ~100-fold excess of the artificial substrate in our assay conditions. Thus, we can rule out that we underestimate the GBA2 activity using our assay conditions.

Deficiency of GBA1 in Gaucher patients causes the accumulation of two sphingolipids, GlcCer and GlcSph (7,12). It has been proposed that under chronic conditions, both, GlcCer and GlcSph, spill-over from the lysosome into the cytoplasm, thereby becoming substrates for GBA2, which degrades GlcCer and GlcSph to glucose and ceramide or sphingosine, respectively (12). We determined the levels of sphingosine and GlcSph in wild-type and GBA1-deficient fibroblasts after separating the membrane and cytosolic fraction (Fig. 4A-B). Both sphingosine and GlcSph levels displayed an elevating trend in membrane fractions of Gaucher disease or GBA1-deficient fibroblasts, respectively (Fig. 4A-B).

We therefore hypothesized that cells accumulating GlcCer and GlcSph, due to a loss of GBA1 activity, might have developed a mechanism, whereby GBA2 activity is diminished to avoid a cytotoxic accumulation of sphingosine or GlcSph. The simplest scenario that could be envisioned in this regard is a direct regulation of GBA2 activity by these metabolites. To test this hypothesis, we first analyzed whether the GBA2 activity is sensitive to sphingosine. CHO cells stably over-expressing mGBA2 were incubated with 20 µM sphingosine complexed to BSA, and GBA1 and GBA2 activity was measured (Fig. 4C-D). The activity of both, GBA1 and GBA2, was significantly reduced to around 27% and 46% of the non-treated samples, respectively (Fig. 4C-D). However, this experimental set up does not allow to conclude whether both GBA1 and GBA2 are sensitive to sphingosine as a sphingosine-dependent reduction of GBA1 activity would be sufficient to reduce GBA2 activity. Thus, to study the effect of sphingosine on GBA2 in a GBA1-independent manner, we incubated embryonal fibroblasts from GBA1-deficient mice with 20 µM sphingosine (Fig. 4E). Sphingosine treatment reduced the GBA2 activity in wild-type fibroblasts to around 62% compared to the non-treated samples (Fig. 4E). Likewise, in GBA1-deficient cells, sphingosine further reduced the residual GBA2 activity to only 6% compared to 14% in the non-treated control (Fig. 4E). Thus, the activity of GBA1, as has been demonstrated before (20,21), but also GBA2 is sensitive to sphingosine. To investigate whether the sphingosine-dependent change in GBA2 activity only occurs in intact cells or also in an *in vitro* system, we prepared hypotonic lysates from mouse brain and incubated them with 20 µM sphingosine for 1.5 h before performing the assay. Both, the activity of GBA1 and GBA2, was reduced after sphingosine treatment compared to control conditions (Fig. 4F-G). To determine whether decreasing the levels of sphingosine reverses inhibition of GBA2 activity, we incubated wild-type and GBA1-deficient cells with the ceramidase inhibitor carmofur. In the presence of carmofur, ceramide levels were increased in the presence of the drug, whereas levels of sphingobases were reduced (Fig. 4H-I). In wild-type cells, carmofur had no effect on GBA2 activity. However, in GBA1-deficient cells, where GBA2 activity is reduced, the inhibition was reversed in the presence of carmofur (Fig. 4J). Carmofur had no direct effect on GBA2 activity when adding the drug to protein lysates in the assay (Fig. 4K).

To further investigate whether sphingosine exerts a direct effect on GBA2 or whether other cellular components indirectly mediate the inhibition of sphingosine on GBA2 activity, we expressed mGBA2 in *E.coli* (Fig. 5A inset). Of note, *E.coli* does not display any GBA1 activity (Fig. 5A), as shown by measuring beta-glucosidase activity at pH 4. Thus, CBE was omitted in this assay. At pH 6 after IPTG induction, bacterial lysates over-expressing GBA2 displayed a prominent beta-glucosidase activity that was blocked by NB-DNJ, demonstrating that GBA2 is expressed and active (Fig. 5A). The dose-response relationship of GBA2 activity to NB-DNJ at pH 6 in *E.coli* lysates displayed an IC_{50} of 14.5 ± 2.7 nM (Fig. 5B), which is very similar to the IC_{50} determined in brain lysates (20.9 ± 1.3 nM) (13). We then assayed the dose-response relationship of GBA2 for sphingosine in bacterial lysates. Sphingosine reduced the GBA2 activity with an IC_{50} of 25.0 ± 0.2 µM (Fig. 5C). These results indicate that sphingosine directly inhibits GBA2.

However, as described above, not only sphingosine, but also GlcSph accumulates in the absence of GBA1. In fact, GlcSph blocked GBA2 activity in a dose-dependent manner with an IC_{50} of 1.5 ± 0.1 µM (Fig. 5D). These results demonstrate that both toxic metabolites, GlcSph and sphingosine, inhibit GBA2 activity.

Structural requirements for the sphingosine-dependent GBA2 inhibition - Next, we tested other sphingolipid metabolites, structurally similar to sphingosine, regarding their ability to inhibit GBA2 activity. In the cell, sphingosine can be phosphorylated by sphingosine kinases to sphingosine-1-phosphate (S1P), a sphingoid messenger that controls multiple signaling pathways (22). S1P structurally differs from sphingosine, as it bears a negatively charged phosphate headgroup. S1P did not inhibit GBA2 activity, suggesting that the presence of a phosphate group disturbs the sphingosine-dependent inhibition of GBA2 activity (Fig. 5E). Fingolimod, or FTY720, is structurally related to sphingosine and is approved for the treatment of Multiple Sclerosis (23). FTY720 carries an octylphenyl group in its carbon tail, while sphingosine itself only bears a double bond at C4. *In vivo*, FTY720 is phosphorylated to form FTY720-phosphate, which resembles naturally occurring S1P and also binds to S1P-surface receptors of cells (24). FTY720 inhibited GBA2 activity with an IC_{50} value of 18.6 ± 0.4 µM (Fig. 5F). Next, we tested whether GBA2 is sensitive to the double bond in the alkyl chain of sphingosine or whether the saturated form of this sphingoid base, sphinganine, also exhibits an inhibitory effect. Sphinganine inhibits GBA2 with an IC_{50} of 30.6 ± 4.5 µM (Fig. 5G), suggesting that the presence of the double bond in the sphingoid alkyl chain is irrelevant for the inhibitory effect. Finally, we investigated whether GBA2 is sensitive to ceramide, a metabolite of sphingosine. However, ceramide (C6, C8, C18) concentrations of up to 300 µM did not diminish GBA2 activity (Fig. 5H-J). Thus, GBA2 seems to be only sensitive to non-acetylated sphingoid bases and their derivatives (GlcSph, sphingosine, sphinganine, FTY720) and not to complex sphingolipids such as ceramides.

Sphingosine reversibly blocks GBA2 activity and follows the rule of mixed-type inhibition - To further characterize the sphingosine-dependent inhibition of GBA2 activity, we tested whether the block is reversible. Hypotonic lysates from bacteria expressing mGBA2 were pre-incubated with 25 µM sphingosine to evoke a half-maximal block of GBA2 activity or with DMSO as a control. After incubation, samples were diluted to a final sphingosine concentration of 3.85 µM. As a control, the sphingosine concentration was maintained at 25 µM. Treatment with 25 µM sphingosine reduced GBA2 activity to 50% of the control values, whereas almost full GBA2 activity was recovered when sphingosine was diluted to 3.85 µM (Fig. 6A). These results indicate that sphingosine reversibly blocks GBA2 activity. To determine the type of reversible inhibition (competitive, non-competitive, uncompetitive, mixed inhibition), we incubated lysates from bacteria over-expressing mGBA2 with 25 µM sphingosine, competed the inhibitory effect by adding increasing amounts of 4-MUG, and analyzed the enzyme activities according to Michaelis-Menten (Fig. 6B). The maximal GBA2 activity (V_{max}) in the presence of sphingosine was reduced to about 50% of the control activity (3.5 ± 0.1 rfu/min *versus* 1.9 ± 0.1 rfu/min, n = 3), pointing towards a non-competitive inhibition of sphingosine for GBA2 (Fig. 6B). Interestingly, the K_m value was also shifted towards higher concentrations (171.3 ± 13.8 µM *versus* 304.0 ± 44.3 µM, n = 3) in the presence of sphingosine (Fig. 6B), which does not resemble the classic non-competitive inhibition model. Thus, our data suggest that the inhibition of GBA2 by sphingosine follows the rules of mixed inhibition, where the inhibitor can bind to an allosteric site of the enzyme if it has not bound its substrate yet, as well as to the enzyme-substrate complex. In this case, the K_m value is increased, which resembles a lower affinity of the enzyme for its substrate, and V_{max} is decreased.

DISCUSSION

Here, we provide new insights into the regulation of GBA2 activity, in particular in Gaucher disease. We demonstrate that GBA2 activity depends on GBA1 activity, but not *vice versa*. This mechanism applies generally - whenever GBA1 was pharmacologically blocked or genetically deleted, and in every *in vitro* and *in vivo* system that we tested, GBA2 activity was reduced. Other reports have also analyzed GBA2 activity in Gaucher disease, but demonstrated an increase in GBA2 activity in brain from GBA1-deficient mice and in fibroblasts from Gaucher disease patients (17,18). These results are in contrast to our findings, and the reason for this discrepancy is not known. One explanation could be a difference in the experimental set-up, that is, how GBA2 activity was measured. Of note, our experiments and the experiments of others (17,18)

were all performed using the artificial, water-soluble substrate 4-MUG and not using the natural lipid GlcCer, making it difficult to directly transfer the molecular mechanisms to the *in vivo* situation. However, we have comprehensively analyzed GBA2 expression and activity in different *in vitro* and *in vivo* models. In none of them GBA2 expression or activity were higher in the absence of GBA1 activity, arguing against earlier findings described above.

Our results indicate that GBA2 activity is inhibited by the cytotoxic metabolites sphingosine and GlcSph through direct binding. It has been proposed that sphingosine is generated by GBA2-dependent hydrolysis of GlcSph (12), whose levels are dramatically increased in Gaucher disease patients (6). GlcSph is generated by intralysosomal deacylation of the accumulating GlcCer and leaves the lysosome through a yet unknown mechanism (7). We first determined sphingosine levels in fibroblasts from control and Gaucher patients using mass spectrometry: sphingosine levels were slightly, albeit not significantly, increased in Gaucher fibroblasts with 1.3 ± 0.8 pmol/µg protein in type I samples, 2.2 ± 2.3 pmol/µg protein in type II samples, and 1.2 ± 0.51 pmol/µg protein in type III samples compared to 1.4 ± 0.6 pmol/µg protein in control cells. However, after separating the cells into a membrane and cytosolic fraction, sphingosine levels in the membrane fraction of all three types of Gaucher disease showed an elevating trend (Fig. 4A). The IC_{50} of sphingosine for GBA2 is relatively high (25.0 ± 0.2 µM in mGBA2 expressed in bacteria). This concentration will never be reached in a cell without causing cell death. However, the local sphingosine concentration could be much higher than the global concentration in the cell. The concentration is presumably the highest in membranes directly at the site of production, which, according to the model, is close to GBA2. In line with this model, sphingosine accumulates preferably in the membranes of fibroblasts from Gaucher disease patients. To investigate the inhibition of GBA2 activity by sphingosine in a cellular context in more detail, a quantitative subcellular analysis of the sphingosine localization would be needed. Furthermore, GlcSph, as a cationic amphiphile, is highly cytotoxic, and its accumulation has also been attributed to the neuropathological defects in Gaucher disease (10,25,26). We demonstrate that not only sphingosine, but also GlcSph inhibits GBA2 activity. Of note, GBA1 activity has been shown to be inhibited by GlcSph (27). Thus, both cytotoxic metabolites inhibit GBA2 activity in a negative feedback loop to prevent further accumulation.

Direct inhibition of GBA2 activity is the most straightforward explanation to how sphingosine regulates GBA2 activity. However, sphingosine has other properties that could also affect GBA2 activity. Sphingosine is also a "bioactive lipid" (28). It either exerts its effect by directly binding to a protein and/or it indirectly changes the properties of cell membranes and, thereby, protein function. Sphingosine is a surface active agent, which attains its function due to its amphipathic structure: the head group carries an amino and two hydroxyl groups, which represent the hydrophilic part, while the carbon tail is highly hydrophobic. GBA2 activity is sensitive to detergents (13). Sphingosine forms micelles above a critical micelle concentration (cmc) of 1 µM at pH 7.4 (29), close to the calculated IC_{50} for GBA2. Palmitoyl-carnitine is a fatty acyl ester with a cmc of 10 µM (30) and contains similar surfactant properties as sphingosine without being involved in sphingolipid metabolism. Palmitoyl-carnitine also showed a dose-dependent inhibition of GBA2 activity in bacterial lysates with an IC_{50} of 31.31 ± 2.68 µM (data not shown). Thus, palmitoyl-carnitine, but also sphingosine, might act as surfactants, forming protein-detergent complexes with GBA2, dissolving GBA2 from a membrane environment. We have shown that GBA2 is a membrane-associated protein at the cytoplasmic site of the ER and the *cis*-Golgi and that the interaction with the membrane, in particular with phospholipids, is crucial for GBA2 activity. After washing the protein off from the membrane, the activity is dramatically reduced, but can be restored when adding back membranes (13). Thus, dissolving GBA2 from the membrane by forming protein-detergent complexes would diminish its activity.

In conclusion, we reveal a sphingosine-dependent regulation of GBA2 activity, which occurs in the absence of GBA1 activity and might also occur in Gaucher disease. Our results add a new chapter to the understanding of the molecular mechanism underlying Gaucher disease pathology, presenting new ideas for the therapy of this severe lysosomal storage disorder.

EXPERIMENTAL PROCEDURES

Constructs – The open reading frame of mouse GBA2 (NM_172692) or mGBA1 (NM_001077411.2) was amplified from cDNA using primers containing restriction sites and a Kozak sequence in front of the start codon. The sequence encoding a hemagglutinin (HA) tag was

added by PCR at the 3'-end. PCR products were subcloned either into pcDNA3.1 or pcDNA6 (Invitrogen) and their sequence was verified. mGBA2-HA was cloned into an expression vector that additionally expresses eGFP. For expression in *E.coli*, a His_6-tag was added to the 3'-end of mGBA2 and the construct was cloned into the pET21a vector (Novagen).

Cell lines and culture – Detailed information about the different cell lines used in this study can be found in Table 1. Cell lines from Gaucher and control patients were obtained from Coriell or from TeleThon (31). Mouse embryonic fibroblasts from wild-type and GBA1- or GBA2-deficient mice have been described elsewhere (13). Human fibroblasts were cultured in DMEM, 100 mM sodium pyruvate, 200 mM L-glutamine (all Thermo Fisher Scientific), 15% FCS (Biochrom); HAP1 cells were cultured in IMDM, 70 IU/ penicillin, 70 µg/ml streptomycin (all Thermo Fisher Scientific), 10% FCS; stable HEK293 cell lines were cultured in MEM, 1x non-essential amino acids, 1 mg/ml G418 (all Thermo Fisher Scientific), 10% FCS; HeLa delta SGPL1 and mouse embryonic fibroblasts were cultured in DMEM, 100 mM sodium pyruvate, 200 mM L-glutamine, 70 IU/ penicillin, 70 µg/ml streptomycin (all Thermo Fisher Scientific), 10% FCS; CHO single or double stable cell lines were cultured in F12, 1 mg/ml G418 and/or 0.01 mg/ml blasticidin (all Thermo Fisher Scientific), 10% FCS. All cells were kept at 37 °C with 5% or 7.5% CO_2. Cells were transfected using polyethylenimine (PEI, Sigma Aldrich). The generation of stable cell lines is described elsewhere (13).

Mice – All animal experiments were conducted according to the German law of animal protection and in agreement with the approval of the local institutional animal care committees (Landesamt für Natur, Umwelt und Verbraucherschutz, North Rhine-Westphalia). Frozen brain tissue from wild-type and CBE-treated mice was obtained from the Futerman lab, Weizman Institute of Science, Israel (15). Mice were maintained under specific pathogen-free conditions in the Experimental Animal Center of the Weizmann Institute of Science, and they were handled according to protocols approved by the Weizmann Institute Animal Care Committee according to international guidelines. The generation of GBA2-deficient mice has been described elsewhere (32).

Antibodies – Antibodies are listed in Table 3. The polyclonal GBA2 antibody was generated by immunizing rabbits (experiments performed by Davids Biotechnology) with the full-length mGBA2 protein expressed in *E.coli* and purified from inclusion bodies (see below).

Purification of recombinant GBA2 from E.coli inclusion bodies to generate polyclonal antibodies - All steps were performed at 4 °C. Buffers contained protease inhibitor mixture Complete (Roche Life Science). Cells were re-suspended and lysed by sonication (3 x 30 s, Branson sonifier) in 50 mM Tris/HCl, pH 8.0, 200 µg/ml lysozyme, DNAse 1000 U/l culture, 500 mM NaCl, 5 mM $MgCl_2$ and 1 mM DTT. After a 20 min incubation on ice, the suspension was centrifuged for 30 min at 11,000 x g and 4 °C. The pellet was re-suspended in solubilization buffer containing 1% Triton-X 100 and 50 mM Tris/HCl, pH 8.0, 0.2 mM EDTA, and 1 mM DTT. The suspension was incubated by end-over-end rotation for 20 min and centrifuged for 15 min at 15,000 x g and 4 °C. The pellet containing the GBA2 inclusion bodies was re-extracted twice in the same way. GBA2 was solubilized from the inclusion bodies by sonification (3 x 30 s, Branson sonifier) in buffer L containing 20 mM imidazol, 20 mM Na-phosphate, 500 mM NaCl, 7 M urea, pH 7.0 and loaded onto a $CoCl_2$-activated HisTrap column (GE Healthcare Life Sciences) equilibrated with buffer L. The column was washed with 10 column volumes buffer L. Recombinant GBA2 was eluted with buffer L containing 500 mM imidazole, collected, and concentrated to ~1.5 mg/ml using an Amicon Ultra-15 Centrifugal Filter Unit with Ultracel-50 membrane (Merck Millipore).

Affinity purification of polyclonal GBA2 antibody - Recombinant full-length GBA2 (1.5 mg) was loaded onto a 7.5% SDS-Gel using a SE400 electrophoresis unit (Hoefer). The gel slice containing mGBA2 was cut out and transferred to a PVDF membrane by Western blotting. The blot was incubated for 2 h with 20 ml of the final bleed (rabbit serum), which was diluted with 1 volume TBS. The blot was washed consecutively with TBS, with TBS containing 0.05% Tween20 (TBST), with 20 mM Tris/HCl, pH 7.4, and with 20 mM Tris/HCl, pH 7.4, 500 mM NaCl. Acidic elution was performed by consecutive incubation with 0.1 M glycine at pH 2.5 and at pH 1.9. Alkaline elution was next performed with 0.1 M triethylamine (TEA), pH 11.5. Acidic eluates were neutralized with 1 M Tris/HCl, pH 8.8, alkaline elutes with 1 M Tris/HCl, pH 7.4. Eluates were pooled and concentrated using an Amicon Ultra-15 Centrifugal Filter Unit with Ultracel-50

membrane (Merck Millipore) to produce antibody GBA2-4/5.

Quantitative real-time PCR – RNA was isolated using the NucleoSpinII columns (Macherey-Nagel) according to the manufacturer's protocol. Reverse transcription was performed using Superscript III (Thermo Scientific Fisher) and 2 µg RNA. Quantitative real-time PCR (qPCR) was performed using SYBR green (Biorad) in a BioRad I-cycler with an IQ5 optical system. Primers are listed in Table 2. Data was analyzed using the BioRad IQ5 optical system software and calculated according to the delta-delta-CT method (Biorad Bulletin). After running the cycles, a melt-curve analysis was performed to detect non-specifically amplified products. mRNA expression-levels were normalized to the mean of the housekeeping genes (hB2m, hAlas1).

Protein preparation – All steps were performed at 4 °C in the presence of a mammalian protease inhibitor cocktail (mPIC, Sigma Aldrich). Tissues were homogenized in hypotonic buffer (10 mM HEPES, 0.5 mM EDTA, pH 7.4; 0.1 g/ml wet weight) using an Ultra-turrax (IKA) and three pulses (20 s each) of sonification in ice-cold water (Branson sonifier). Tissue suspensions (total lysate) were subjected to low speed centrifugation for 20 min at 1,000 x g. The supernatant (PNS, post-nuclear supernatant) was used for activity assays (13). Cultured cells were washed once with PBS and harvested using 1 ml PBS/EDTA per 9 cm cell culture dish and cells were pelleted for 5 min at 600 x g and 4 °C. Afterwards, the pellets were directly lysed in hypotonic buffer, sonicated, and used for activity assays or Western blot analysis. Proteins were de-glycosylated using PNGase F (New England Biolabs) according to the manufacturer's protocol. Protein concentration was determined using the Bradford assay or the bicinchoninic acid (BCA) test kit (Pierce) according to the manufacturer's protocol.

Western blot analysis – Western blot analysis was performed as described elsewhere (13,33).

Beta-glucosidase activity assay – The assay was performed as described elsewhere (13). In brief, the activity of cellular GBAs was analyzed using 4-methylumbelliferyl-beta-D-glucopyranoside (4-MU-beta-D-glucopyranoside, 4-MUG, Sigma Aldrich) as a fluorescent substrate (1.67 mM final) at pH 4 and pH 6. Cleavage of 4-MUG was monitored in real-time in 384-well plates in a Fluostar Omega reader (BMG labtech) at 29 °C using the filter pair 355 nm/460 nm for excitation and emission, respectively. To discriminate between GBA1 and GBA2 activity, CBE (Conduritol B epoxide, Sigma Aldrich), an inhibitor of GBA1 (34), or NB-DNJ (*N*-butyldeoxynojirimycin, Sigma Aldrich), an inhibitor of GBA2 (16), was included. The pH of the lysates and of the 4-MUG solution was adjusted by diluting with McIlvaine buffer. We defined the activity of GBA1 as the CBE-blockable activity at pH 4 and the activity of GBA2 as the NB-DNJ-blockable activity at pH 6. The hydrolysis of 4-MUG was recorded as a change in relative fluorescence units (rfu) per hour. Each analysis was performed as a quadruplicate in parallel.

Treatments – Cells on culture plate were treated with CBE (25 µM, Sigma Aldrich, C5424), NB-DNJ (2 µM, Enzo Life Sciences, BML-SL230), or carmofur (2.9 µM, Cayman Chemical, #14243) in culture medium at 37 °C for 48 h before analyzing the beta-glucosidase activity. As a control, the GBA2 activity in lysates from non-treated cells was analyzed in presence of 2.9 µM carmofur to exclude a direct effect on GBA2. To prepare lipid-BSA complexes, a 4 mg/ml BSA solution was prepared in PBS (pH 7.4). The lipid stocks were diluted in the 4 mg/ml BSA solution to the desired concentration. Lipid-BSA complexes were produced by sonicating for 2 min (Branson sonifier), resulting in a milky suspension. The following lipids were used: sphingosine (Sigma Aldrich, #1802), sphinganine (Avanti Polar Lipids, #860498P), FTY720 (Sigma Aldrich, SML0700), sphingosine-1-phosphate (Avanti Polar Lipids, #860492P), C6 ceramide (Enzo Life Sciences, BML-SL110), C8 ceramide (Enzo Life Sciences, BML-SL112), C18 ceramide (Matreya LLC, #1832). Cells were treated with lipid-BSA complexes diluted in culture medium containing only 1% FCS at 37 °C for 4.5 h. Hypotonic lysates were incubated with lipid-BSA complexes at RT for 1 h prior to analysis of beta-glucosidase activity.

In vivo experiments – Treatment of mice with CBE has been described elsewhere (15). Frozen brains were taken from this study and used for the experiments presented here.

GBA2 expression in bacteria – Expression of pET21a-mGBA2-His was performed in the *E.coli* strain BL21 Codon Plus (DE3) RIPL (Agilent Technologies, Santa Clara, USA) at 37 °C for 3 h after induction with 1 mM IPTG. mGBA2-His *E.coli* cultures were centrifuged for 10 min at 11,000 x g and 4 °C and the pellet from 30 ml culture was re-suspended in 4.8 ml hypotonic buffer (1:8 dilution of the initial

volume). The cell suspension was sonicated 3 x 20 s in ice-cold water (Branson sonifier) and 20 µl of the protein lysate were used per reaction if not otherwise stated.

Preparation of membrane and soluble fractions for mass spectrometry - Cells were lysed in cold buffer A (10 mM NaCl, 25 mM HEPES pH 7.5, 2 mM EDTA, 1:500 mPic) and incubated on ice for 15 min. The protein concentration was determined by BCA. To separate the soluble from the membrane fraction, samples were centrifuged for 30 min at 100,000 x g at 4 °C (TLA-55, Beckmann). The supernatant was transferred into a fresh tube and the membrane pellet was re-suspended in the same volume of buffer B (200 mM NaCl, 50 mM HEPES pH 7.5, 1:500 mPic).

Quantification of sphingolipids by mass spectrometry – Cells were lysed in hypotonic lysis buffer and used for lipid extraction. Alternatively, the lysate was used for separation of membrane and soluble fractions as described above prior to lipid extraction. Lipids were extracted by adding 500 µl chloroform/methanol/formic acid (1:1:0.1, v/v/v) and thorough mixing (33). At this point, internal standards were added (35). 250 µl of 1 M KCl/0.2 M H_3PO_4 were added, samples were vortexed, and centrifuged at 5,000 rpm for 3 min to obtain phase separation. The lower phase containing the lipids was transferred to a fresh glass vial and the remaining samples were re-extracted by adding 500 µl of chloroform/methanol in a ratio of 2:1 (v/v). Samples were vortexed, centrifuged at 5,000 rpm for 3 min, and the lower phase was combined with the previous extract. Solvents were evaporated under N_2 flow and lipids re-suspended in 500 µl of pure chloroform. Small silica columns (Strata-1-Silica, 55 µM, 70 Å containing 100 mg silica) were equilibrated by flushing with pure chloroform for three times. Afterwards, samples dissolved in pure chloroform were applied and non-polar lipids (e.g. triacylglycerol, sterols) were eluted with three column volumes of pure chloroform. Hexosylceramides, ceramides, glycosylated long chain bases (e.g. GlcSph), and free long chain bases were eluted with three column volumes of acetone/isopropanol (1:1, v/v). The acetone/isopropanol fraction was dried under N_2 flow and dissolved in 100 µl methanol. 50 µl of the sample were dried once more and dissolved in 100 µl chloroform/methanol/300 mM ammonium acetate (300:665:35, v/v/v) (36) and subjected to mass spectrometric analysis by nanospray direct infusion Q-TOF MS/MS as described elsewhere (33,35). The remaining 50 µl of the sample were used for analysis of glycosylated long chain bases using LC-MS/MS with conditions as described elsewhere (37). The relative amounts of the glycosylated long chain bases were determined using d17:1-long chain base as internal standard.

Statistical analysis – Results are presented as mean ± S.D. Statistical analysis was performed using Origin Pro 9.0 (one-way ANOVA). P values are only indicated when considered significant (≤ 0.05).

Acknowledgements. We thank J.H. Krause, S. Sonnenburg, D. Herborn, M. Völker, and I. Lux for technical assistance, Wolfgang Bönigk for cloning, and J.F. Jikeli for help with the analysis. The project was supported by grants from the Deutsche Forschungsgemeinschaft (DFG): SFB645 (to DW, CT, PD), TRR83 (to CT, BB, KS), and the Excellence Cluster ImmunoSensation, Bonn (to DW). A.H. Futerman is the Joseph Meyerhoff Professor of Biochemistry at the Weizmann Institute of Science.

Conflict of interest. The authors declare no competing financial interests.

Author contributions. DW conceived and coordinated the study and wrote the paper. SS designed, performed, and analyzed the experiments and wrote the paper. HGK generated and characterized antibodies and contributed to the design of the experiments, AP, AR, PH, BB, BB, KS, CT, DR, MJG and AHF contributed to the conception and design of the experiments, KG and PD performed and analyzed the lipid contents by mass spectrometry, and HZ and AV performed the CBE-treatments of mice. All authors reviewed the results and approved the final version of the manuscript.

References

1. Brady, R. O., Kanfer, J. N., and Shapiro, D. (1965) Metabolism of Glucocerebrosides. Ii. Evidence of an Enzymatic Deficiency in Gaucher's Disease. *Biochem. Biophys. Res. Commun.* **18**, 221-225
2. Hruska, K. S., LaMarca, M. E., Scott, C. R., and Sidransky, E. (2008) Gaucher disease: mutation and polymorphism spectrum in the glucocerebrosidase gene (GBA). *Hum. Mutat.* **29**, 567-583
3. Pastores, G. M. (1997) Gaucher's Disease. Pathological features. *Baillieres Clin. Haematol.* **10**, 739-749
4. Futerman, A. H., Zimran, A., and (eds.). (2006) *Gaucher disease* CRC Press, Taylor and Francis Group, Boca Raton, FL
5. Meivar-Levy, I., Horowitz, M., and Futerman, A. H. (1994) Analysis of glucocerebrosidase activity using N-(1-[14C]hexanoyl)-D-erythroglucosylsphingosine demonstrates a correlation between levels of residual enzyme activity and the type of Gaucher disease. *Biochem. J.* **303** 377-382
6. Dekker, N., van Dussen, L., Hollak, C. E., Overkleeft, H., Scheij, S., Ghauharali, K., van Breemen, M. J., Ferraz, M. J., Groener, J. E., Maas, M., Wijburg, F. A., Speijer, D., Tylki-Szymanska, A., Mistry, P. K., Boot, R. G., and Aerts, J. M. (2011) Elevated plasma glucosylsphingosine in Gaucher disease: relation to phenotype, storage cell markers, and therapeutic response. *Blood* **118**, e118-127
7. Ferraz, M. J., Marques, A. R., Gaspar, P., Mirzaian, M., van Roomen, C., Ottenhoff, R., Alfonso, P., Irun, P., Giraldo, P., Wisse, P., Sa Miranda, C., Overkleeft, H. S., and Aerts, J. M. (2016) Lyso-glycosphingolipid abnormalities in different murine models of lysosomal storage disorders. *Mol. Genet. Metab.* **117**, 186-193
8. Korkotian, E., Schwarz, A., Pelled, D., Schwarzmann, G., Segal, M., and Futerman, A. H. (1999) Elevation of intracellular glucosylceramide levels results in an increase in endoplasmic reticulum density and in functional calcium stores in cultured neurons. *J. Biol. Chem.* **274**, 21673-21678
9. Nilsson, O., and Svennerholm, L. (1982) Accumulation of glucosylceramide and glucosylsphingosine (psychosine) in cerebrum and cerebellum in infantile and juvenile Gaucher disease. *J. Neurochem.* **39**, 709-718
10. Orvisky, E., Park, J. K., LaMarca, M. E., Ginns, E. I., Martin, B. M., Tayebi, N., and Sidransky, E. (2002) Glucosylsphingosine accumulation in tissues from patients with Gaucher disease: correlation with phenotype and genotype. *Mol Genet Metab* **76**, 262-270
11. Elleder, M. (2006) Glucosylceramide transfer from lysosomes--the missing link in molecular pathology of glucosylceramidase deficiency: a hypothesis based on existing data. *J. Inherit. Metab. Dis.* **29**, 707-715
12. Mistry, P. K., Liu, J., Sun, L., Chuang, W. L., Yuen, T., Yang, R., Lu, P., Zhang, K., Li, J., Keutzer, J., Stachnik, A., Mennone, A., Boyer, J. L., Jain, D., Brady, R. O., New, M. I., and Zaidi, M. (2014) Glucocerebrosidase 2 gene deletion rescues type 1 Gaucher disease. *Proc. Natl. Acad. Sci. USA* **111**, 4934-4939
13. Körschen, H. G., Yildiz, Y., Raju, D. N., Schonauer, S., Bönigk, W., Jansen, V., Kremmer, E., Kaupp, U. B., and Wachten, D. (2013) The non-lysosomal beta-glucosidase GBA2 is a non-integral membrane-associated protein at the endoplasmic reticulum (ER) and Golgi. *J. Biol. Chem.* **288**, 3381-3393
14. Farfel-Becker, T., Vitner, E. B., and Futerman, A. H. (2011) Animal models for Gaucher disease research. *Dis. Model Mech.* **4**, 746-752
15. Vardi, A., Zigdon, H., Meshcheriakova, A., Klein, A. D., Yaacobi, C., Eilam, R., Kenwood, B. M., Rahim, A. A., Massaro, G., Merrill, A. H., Jr., Vitner, E. B., and Futerman, A. H. (2016) Delineating pathological pathways in a chemically induced mouse model of Gaucher disease. *J. Pathol.* **239**, 496-509
16. Ridley, C. M., Thur, K. E., Shanahan, J., Thillaiappan, N. B., Shen, A., Uhl, K., Walden, C. M., Rahim, A. A., Waddington, S. N., Platt, F. M., and van der Spoel, A. C. (2013) beta-Glucosidase 2 (GBA2) activity and imino sugar pharmacology. *J. Biol. Chem.* **288**, 26052-26066

17. Aureli, M., Bassi, R., Loberto, N., Regis, S., Prinetti, A., Chigorno, V., Aerts, J. M., Boot, R. G., Filocamo, M., and Sonnino, S. (2012) Cell surface associated glycohydrolases in normal and Gaucher disease fibroblasts. *J. Inherit. Metab. Dis.* **35**, 1081-1091
18. Burke, D. G., Rahim, A. A., Waddington, S. N., Karlsson, S., Enquist, I., Bhatia, K., Mehta, A., Vellodi, A., and Heales, S. (2013) Increased glucocerebrosidase (GBA) 2 activity in GBA1 deficient mice brains and in Gaucher leucocytes. *J. Inherit. Metab. Dis.* **36**, 869-872
19. Fuller, M., Rozaklis, T., Lovejoy, M., Zarrinkalam, K., Hopwood, J. J., and Meikle, P. J. (2008) Glucosylceramide accumulation is not confined to the lysosome in fibroblasts from patients with Gaucher disease. *Mol. Genet. Metab.* **93**, 437-443
20. Erickson, J. S., and Radin, N. S. (1973) N-hexyl-O-glucosyl sphingosine, an inhibitor of glucosyl ceramide -glucosidase. *J. Lipid. Res.* **14**, 133-137
21. Grabowski, G. A., Dinur, T., Osiecki, K. M., Kruse, J. R., Legler, G., and Gatt, S. (1985) Gaucher disease types 1, 2, and 3: differential mutations of the acid beta-glucosidase active site identified with conduritol B epoxide derivatives and sphingosine. *Am. J. Hum. Genet.* **37**, 499-510
22. Spiegel, S., and Milstien, S. (2003) Sphingosine-1-phosphate: an enigmatic signalling lipid. *Nat. Rev. Mol. Cell. Biol.* **4**, 397-407
23. Brinkmann, V., Billich, A., Baumruker, T., Heining, P., Schmouder, R., Francis, G., Aradhye, S., and Burtin, P. (2010) Fingolimod (FTY720): discovery and development of an oral drug to treat multiple sclerosis. *Nat. Rev. Drug. Discov.* **9**, 883-897
24. Chun, J., and Hartung, H. P. (2010) Mechanism of action of oral fingolimod (FTY720) in multiple sclerosis. *Clin. Neuropharmacol.* **33**, 91-101
25. Schueler, U. H., Kolter, T., Kaneski, C. R., Blusztajn, J. K., Herkenham, M., Sandhoff, K., and Brady, R. O. (2003) Toxicity of glucosylsphingosine (glucopsychosine) to cultured neuronal cells: a model system for assessing neuronal damage in Gaucher disease type 2 and 3. *Neurobiol Dis* **14**, 595-601
26. Sun, Y., Liou, B., Ran, H., Skelton, M. R., Williams, M. T., Vorhees, C. V., Kitatani, K., Hannun, Y. A., Witte, D. P., Xu, Y. H., and Grabowski, G. A. (2010) Neuronopathic Gaucher disease in the mouse: viable combined selective saposin C deficiency and mutant glucocerebrosidase (V394L) mice with glucosylsphingosine and glucosylceramide accumulation and progressive neurological deficits. *Hum Mol Genet* **19**, 1088-1097
27. Sarmientos, F., Schwarzmann, G., and Sandhoff, K. (1986) Specificity of human glucosylceramide beta-glucosidase towards synthetic glucosylsphingolipids inserted into liposomes. Kinetic studies in a detergent-free assay system. *Eur. J. Biochem.* **160**, 527-535
28. Contreras, F. X., Sot, J., Alonso, A., and Goni, F. M. (2006) Sphingosine increases the permeability of model and cell membranes. *Biophys. J.* **90**, 4085-4092
29. Sasaki, H., Arai, H., Cocco, M. J., and White, S. H. (2009) pH dependence of sphingosine aggregation. *Biophys. J.* **96**, 2727-2733
30. Goni, F. M., Requero, M. A., and Alonso, A. (1996) Palmitoylcarnitine, a surface-active metabolite. *FEBS Lett.* **390**, 1-5
31. Filocamo, M., Mazzotti, R., Corsolini, F., Stroppiano, M., Stroppiana, G., Grossi, S., Lualdi, S., Tappino, B., Lanza, F., Galotto, S., and Biancheri, R. (2014) Cell Line and DNA Biobank From Patients Affected by Genetic Diseases. *Open J. Biores.* **1**, e2
32. Yildiz, Y., Matern, H., Thompson, B., Allegood, J. C., Warren, R. L., Ramirez, D. M., Hammer, R. E., Hamra, F. K., Matern, S., and Russell, D. W. (2006) Mutation of beta-glucosidase 2 causes glycolipid storage disease and impaired male fertility. *J. Clin. Invest.* **116**, 2985-2994
33. Raju, D., Schonauer, S., Hamzeh, H., Flynn, K. C., Bradke, F., Vom Dorp, K., Dormann, P., Yildiz, Y., Trotschel, C., Poetsch, A., Breiden, B., Sandhoff, K., Korschen, H. G., and Wachten, D. (2015) Accumulation of glucosylceramide in the absence of the beta-glucosidase GBA2 alters cytoskeletal dynamics. *PLoS Genet.* **11**, e1005063
34. Legler, G., and Bieberich, E. (1988) Active site directed inhibition of a cytosolic beta-glucosidase from calf liver by bromoconduritol B epoxide and bromoconduritol F. *Arch. Biochem. Biophys.* **260**, 437-442
35. Ginkel, C., Hartmann, D., vom Dorp, K., Zlomuzica, A., Farwanah, H., Eckhardt, M., Sandhoff, R., Degen, J., Rabionet, M., Dere, E., Dormann, P., Sandhoff, K., and Willecke, K. (2012)

Ablation of neuronal ceramide synthase 1 in mice decreases ganglioside levels and expression of myelin-associated glycoprotein in oligodendrocytes. *J. Biol. Chem.* **287**, 41888-41902

36. Welti, R., Li, W., Li, M., Sang, Y., Biesiada, H., Zhou, H. E., Rajashekar, C. B., Williams, T. D., and Wang, X. (2002) Profiling membrane lipids in plant stress responses. Role of phospholipase D alpha in freezing-induced lipid changes in Arabidopsis. *J. Biol. Chem.* **277**, 31994-32002
37. Scherer, M., Leuthäuser-Jaschinski, K., Ecker, J., Schmitz, G., and Liebisch, G. (2010) A rapid and quantitative LC-MS/MS method to profile sphingolipids. *J. Lipid Res.* **51**, 2001-2011

Footnotes. The abbreviations used are: CBE, conduritol B epoxide; FTY720, 2-amino-2-[2-(4-octylphenyl)ethyl]) propane-1,3-diol; GBA1, acid beta-glucosidase, GBA2, non-lysosomal beta-glucosidase; GlcCer, glucosylceramide; GlcSph, glucosylsphingosine; NB-DNJ, *N*-butyl-deoxynojirimycin; S1P, sphingosine-1-phosphate; 4-MUG, 4-methyl-umbelliferyl beta-D-glucopyranoside; CHO, Chinese hamster ovary cell line; DMEM, Dulbecco's Modified Eagle Medium; F12, Ham's F-12 Nutrient Mix; FCS, fetal calf serum; HAP1, human fibroblast-like cells; HeLa, immortalized cervical cancer cells originating from Henrietta Lacks; hFB, human fibroblast; IPTG, isopropyl beta-D-1-thiogalactopyranoside; MEM, Minimum Essential Medium; OptiMEM, reduced Serum Medium; mPic, mammalian protease inhibitor cocktail; Sph, sphingosine.

Figure legends

Figure 1: GBA2 activity is down-regulated in the absence of GBA1. A. GBA1 activity in fibroblasts from control and Gaucher patients. GBA1 activity was measured in hypotonic lysates from control (ctrl) and Gaucher fibroblasts (type I, II, III) using 1.67 mM 4-MUG as a substrate. Data were normalized to the control. 100% GBA1 activity: 32.3 pmol/µg protein/h. **B.** see A. for GBA2 activity. 100% GBA2 activity: 0.9 pmol/µg protein/h. **C.** GBA1 activity in wild-type (WT) and GBA1-deficient (KO) HAP1 fibroblasts. GBA1 activity was measured in hypotonic lysates using 1.67 mM 4-MUG; two independent GBA1-deficient cell lines (#001, #010) were analyzed. Data were normalized to wild-type cells. 100% GBA1 activity: 8.9 pmol/µg protein/h. **D.** see C for GBA2 activity. 100% GBA2 activity: 2.2 pmol/µg protein/h. **E.** see C for wild-type (WT) and GBA2-deficient (KO) HAP1 fibroblasts. GBA1 activity: 7.4 pmol/µg protein/h. **F.** see E for GBA2 activity. 100% GBA2 activity: 2.2 pmol/µg protein/h. **G.** GBA1 mRNA expression in control (ctrl) and Gaucher patients (type I, II, III) analyzed by qPCR. Data were normalized to the control. **H.** see G for GBA2. **I.** GBA1 and GBA2 protein in control (ctrl) and Gaucher patients (type I, II). Hypotonic lysates were subjected to Western blot analysis using GBA1- and GBA2-specific antibodies. Calnexin was used as a loading control. **J.** Quantification of GBA1 protein expression levels, normalized to the loading control and then to control samples. For quantification, all GBA1 bands were taken into account. **K.** see J. for GBA2. All data are represented as mean + S.D.; n numbers are indicated in brackets.

Figure 2: GBA2 activity depends on GBA1 activity. A. GBA1 activity in CBE-treated human fibroblasts. GBA1 activity was measured in hypotonic lysates from control (ctrl) and fibroblasts treated with 25 µM CBE for 48 h using 1.67 mM 4-MUG as a substrate. Data were normalized to the control. 100% GBA1 activity: 261.7 pmol/µg protein/h. **B.** see A. for GBA2 activity. 100% GBA2 activity: 6.0 pmol/µg protein/h. **C.** GBA1 activity in CBE-treated HEK293 cells stably over-expressing GBA2. GBA1 activity was measured in hypotonic lysates from control (ctrl) and cells treated with 25 µM CBE for 48 h using 1.67 mM 4-MUG as a substrate. Data were normalized to the control. 100% GBA1 activity: 27.0 pmol/µg protein/h. **D.** see C. for GBA2 activity. 100% GBA2 activity: 206.0 pmol/µg protein/h. **E.** GBA1 activity in CBE-treated GBA1-deficient mouse embryonal fibroblasts. GBA1 activity was measured in hypotonic lysates from wild-type (+), GBA1-deficient (-), CBE-treated GBA1-deficient (± 25 µM CBE, 48 h) mouse embryonal fibroblasts using 1.67 mM 4-MUG as a substrate. Data were normalized to the non-treated wild-type cells. 100% GBA1 activity: 125.9 pmol/µg protein/h. **F.** see E for GBA2 activity. 100% GBA2 activity: 5.5 pmol/µg protein/h. **G.** GBA1 and GBA2 protein expression in control (DMSO-treated) and CBE-treated (CBE, 25 µM, 48 h) HEK293 cells transiently over-expression GBA2. Hypotonic lysates were subjected to Western blot analysis using GBA1- and GBA2-specific (anti-HA) antibodies. Tubulin was used as a loading control for HEK293 cells. CHO cells stably expressing GBA1 and GBA2 were used as positive control. **H.** Quantification of GBA1 and GBA2 protein expression levels in CBE-treated cells (data from H), normalized to control samples. **I.** GBA1 activity in NB-DNJ-treated HEK293 cells transiently over-expressing GBA2. GBA1 activity was measured in hypotonic lysates from control (ctrl) and HEK293 cells treated with 2 µM NB-DNJ for 48 h using 1.67 mM 4-MUG as a substrate. Data were normalized to the control. 100% GBA1 activity: 26.3 pmol/µg protein/h. **J.** see I for GBA2 activity. 100% GBA2 activity: 195.8 pmol/µg protein/h. **K.** Time course of the GBA1-dependent regulation of GBA2 activity in CHO cells stably over-expressing mGBA2. Cells were incubated with 25 µM CBE for 10 min up to 48 h. Beta-glucosidase activity was analyzed in hypotonic cell lysates in presence of 1.67 mM 4-MUG. 100% GBA1 activity: 7.4 pmol/µg protein/h; 100% GBA2 activity: 405.0 pmol/µg protein/h. All data are represented as mean + S.D.; n numbers are indicated in brackets.

Figure 3: GBA2 activity is also reduced *in vivo* in a pharmacological Gaucher mouse model. A. GBA1 activity in brain from CBE-injected mice. GBA1 activity was measured in hypotonic brain lysates from control (PBS) and CBE-injected mice using 1.67 mM 4-MUG as a substrate. Data were normalized to the control. 100% GBA1 activity: 6.2 pmol/µg protein/h. **B.** see A. for GBA2 activity. 100% GBA2 activity: 84.6 pmol/µg protein/h. **C.** GBA1 and GBA2 protein expression in brain from control (PBS) and CBE-injected mice. Hypotonic lysates were subjected to Western blot analysis using GBA1- and GBA2-specific antibodies. Calnexin was used as a loading control. A representative blot for one CBE-concentration and three different animals is shown. CHO cells stably expressing GBA1 and GBA2 were used as positive control. **D.** Quantification of GBA2 protein expression levels in brain from CBE-

injected mice (data from H), normalized to control (PBS) samples. All data are represented as mean + S.D.; n numbers are indicated in brackets.

Figure 4: Sphingosine blocks GBA2 activity. A. Quantitative lipid analysis by mass spectrometry. Ceramide and hexosylceramide levels were determined from total cell lysates, whereas sphingosine levels were determined in membrane fractions from wild-type and Gaucher fibroblasts (ctrl: control fibroblasts, I: type I Gaucher, II: type II Gaucher, III: type III Gaucher); n = 4. **B.** Glucosylsphingosine levels in membranes from wild-type and GBA1-KO HAP1 cells. Data are shown as mean + SEM, n = 4. **C.** GBA1 activity in sphingosine-treated CHO cells stably over-expressing mGBA2. GBA1 activity was measured in hypotonic lysates from cells treated with 20 µM sphingosine for 4.5 h using 1.67 mM 4-MUG as a substrate. Data were normalized to the control (-). 100% GBA1 activity: 33.9 pmol/µg protein/h. **D.** see C. for GBA2. 100% GBA1 activity: 149.9 pmol/µg protein/h. **E.** GBA2 activity in wild-type (WT) and GBA1-deficient embryonal mouse fibroblasts. GBA2 activity was measured in hypotonic lysates from wild-type or GBA1-deficient cells (GBA1-KO) treated with 20 µM sphingosine for 4.5 h using 1.67 mM 4-MUG as a substrate. Data were normalized to the control (-). 100% GBA2 activity: 29.4 pmol/µg protein/h. **F.** GBA1 activity in sphingosine-treated brain lysates. GBA1 activity was measured in hypotonic lysates that were treated with 20 µM sphingosine for 1.5 h using 1.67 mM 4-MUG as a substrate. Data were normalized to the control (-). 100% GBA1 activity: 38.2 pmol/µg protein/h. **G.** see F for GBA2 activity. 100% GBA2 activity: 233.1 pmol/µg protein/h. **H.** Ceramide levels were analyzed using mass spectrometry in total lysates from wild-type and GBA1-KO HAP1 cells treated with DMSO or 2.9 µM carmofur for 48 h. **I.** see H. for sphingobase levels. **J.** GBA2 activity in wild-type (+) and GBA1-KO (-) HAP1 cells. Cell were treated with 2.9 µM carmofur for 48 h before preparing total lysates. **K.** GBA2 activity in the presence of 2.9 µM carmofur. The drug was directly added to the protein lysates when performing the assay.

Figure 5: GBA2 expression and activity in *E.coli*. A. GBA2 expression was induced by 1 mM IPTG and expression was verified by Western blot analysis using an anti-His antibody. Beta-glucosidase activity in bacterial lysates before (-) and after induction with 1 mM IPTG (+) was measured at pH 4 and pH 6. There was no difference in beta-glucosidase activity in the presence or absence of 25 µM CBE at pH 4, demonstrating that there is no endogenous GBA1 activity. The IPTG-induced beta-glucosidase activity at pH 6 is blocked by 8.3 µM NB-DNJ, demonstrating that the activity is conveyed by GBA2. Data represent n = 1. **B.** Dose-response relationship of GBA2 activity to NB-DNJ at pH 6. Maximal activity (2.2 pmol/µg protein/h) has been set to 100%. Grey line represents the exponential fit. **C.** see B. for sphingosine. **D.** see B. for glucosylsphingosine. **E.** see B. for sphingosine-1-phosphate. **F.** see B. for FTY720 (Fingolimod). **G.** see B. for sphinganine. **H.** see B. for C18 ceramide. **I.** see B for C6 ceramide. **J.** see B. for C8 ceramide.

Figure 6: Sphingosine reversibly blocks GBA2 at an allosteric site. A. GBA2 activity after sphingosine treatment. Hypotonic GBA2-expressing bacterial lysates were incubated with 25 µM sphingosine (Sph) for 1 h before diluting the sample, resulting in a sphingosine concentration of 3.85 µM; a control sample was also diluted, but the sphingosine concentration was kept constant at 25 µM. 100% GBA2 activity: 2.2 pmol/µg protein/h. **B.** Dose-response relationship of GBA2 activity to 4-MUG at pH 6 in the absence (ctrl) or presence (25 µM) of sphingosine; n = 3. All data are represented as mean + S.D.; n numbers are indicated in brackets.

Tables

Cell line	Genotype	Supplier	Catalogue #	Disease	Mutation	Patient Sex	Patient Age
hFB 1	control	Coriell	GM00024 C	-	-	M	30 yrs
hFB 2	mutant GBA1	Coriell	GM00372 A	GD type I	84G ins, N370S	M	29 yrs
hFB 3	mutant GBA1	Coriell	GM00852 A	GD type I	84G ins, N370S	M	20 yrs
hFB 4	mutant GBA1	Coriell	GM00877 A	GD type II	L444P, L444P, A456P, V460V	M	1 y
hFB 5	mutant GBA1	Coriell	GM00878	-	L444P, A456P, V460V	F	N/A
hFB 6	mutant GBA1	Coriell	GM01607B	GD type I	N370S, V394L	M	30 yrs
hFB 7	mutant GBA1	Coriell	GM04394	GD type I	L444P	M	1 y
hFB 8	control	Coriell	GM05399 A	-	-	M	1
hFB 9	control	Coriell	GM05757 C	-	-	M	7 yrs
hFB 10	mutant GBA1	Coriell	GM08760	GD type II	L444P	M	1 y
hFB 11	mutant GBA1	Coriell	GM10915 A	GD type I	L444P	M	7 yrs
hFB 12	mutant GBA1	Coriell	GM20272 B	GD type III	L444P	M	N/A
hFB 14	mutant GBA1	Coriell	GM01260	GD type II	L444P, P415R	F	11 m
hFB 15	mutant GBA1	TeleThon	FFF0091977	GD type III	L444P, L444P	N/A	N/A
hFB 16	mutant GBA1	TeleThon	FFF0491979	GD type III	L444P, L444P	N/A	N/A
hFB 17	mutant GBA1	TeleThon	FFF1081981	GD type III	L444P, L444P	N/A	N/A
hFB 18	mutant GBA1	TeleThon	FFF1161982	GD type II	L444P, R257Q	N/A	N/A
hFB 19	mutant GBA1	TeleThon	FFF0181985	GD type II	L444P, R120W	N/A	N/A
hFB 20	mutant GBA1	TeleThon	FFF0591990	GD type III	L444P, F213I	N/A	N/A
HAP1	WT	Horizon	-	WT	-	-	-
HAP1	GBA1-KO	Horizon	HZGHC00278 6c001	GBA1-KO	479 bp insertion in exon 6	-	-
HAP1	GBA1-KO	Horizon	HZGHC00278 6c010	GBA1-KO	1 bp insertion in exon 6	-	-
HAP1	GBA2-KO	Horizon	HZGHC00410 9c001	GBA2-KO	5 bp deletion in exon 1	-	-

HAP1	GBA2-KO	Horizon	HZGHC00410 9c011	GBA2-KO	1 bp insertion in exon 1	-	-

Table 1: Human cell lines.

Gene	Primer	Sequence (5'-3')
hGBA1	C1798	ACAGCCACAGCATCATCACG
	C1799	CATATAGGCATGGGCTTGAG
hGBA2	C1800	CATATAGGCATGGGCTTGAG
	C1801	AGCTGCCAACGACAGAACTG
hB2m	C1818	CGAGACATGTAAGCAGCATC
	C1819	GCAACCTGCTCAGATACATC
hAlas1	C1824	AGCTTCAGGAGGATGTGCAG
	C1825	AGTTCTTCAGCAGTCCACTG

Table 2: Primers used for qPCR.

Primary Antibody	Species	Producer	Catalogue #	Dilution WB
Calnexin	rb	Sigma	C4731	1:40,000 (tissue)
				1:5,000-10,000 (cells)
GBA1	rb	Sigma	G4171	1:1,000
GBA1-2F8/4A12 mix	rt	Körschen et al., 2013	-	1:50
GFP	rb	Abcam	ab6556	1:5,000
His-Tag	ms	Novagen	70796-3	1:1,000
Beta-Tubulin	ms	Sigma	TUB 2.1	1:1,000
HA-Tag	rt	Roche	11867431001	1:5,000
GBA2-4/5	rb	unpublished	-	1:5,000
Secondary Antibody	Species	Producer	Catalogue #	Dilution WB
dk α ms IRDye680LT		LI-COR Biosciences	926-68022	1:20,000
dk α ms IRDye800CW		LI-COR Biosciences	926-32212	1:20,000
dk α rb IRDye680		LI-COR Biosciences	926-32223	1:20,000

dk α rb IRDye800CW	LI-COR Biosciences	926-32213	1:20,000
gt α rt IRDye680	LI-COR Biosciences	926-32229	1:20,000
gt α rt IRDye800CW	LI-COR Biosciences	926-32219	1:20,000

Table 3: Antibodies.

Figures

Figure 1

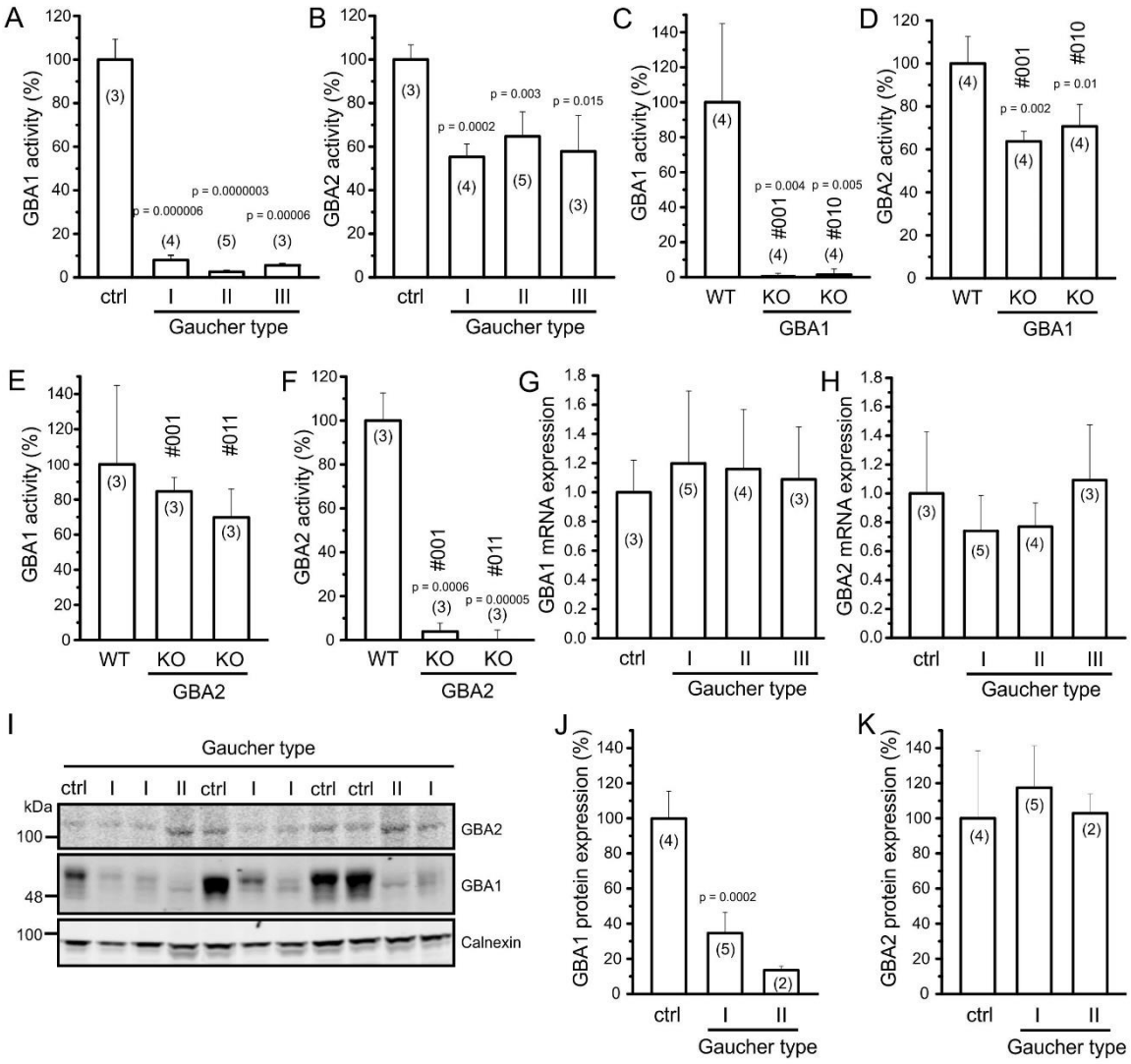

Figure 2

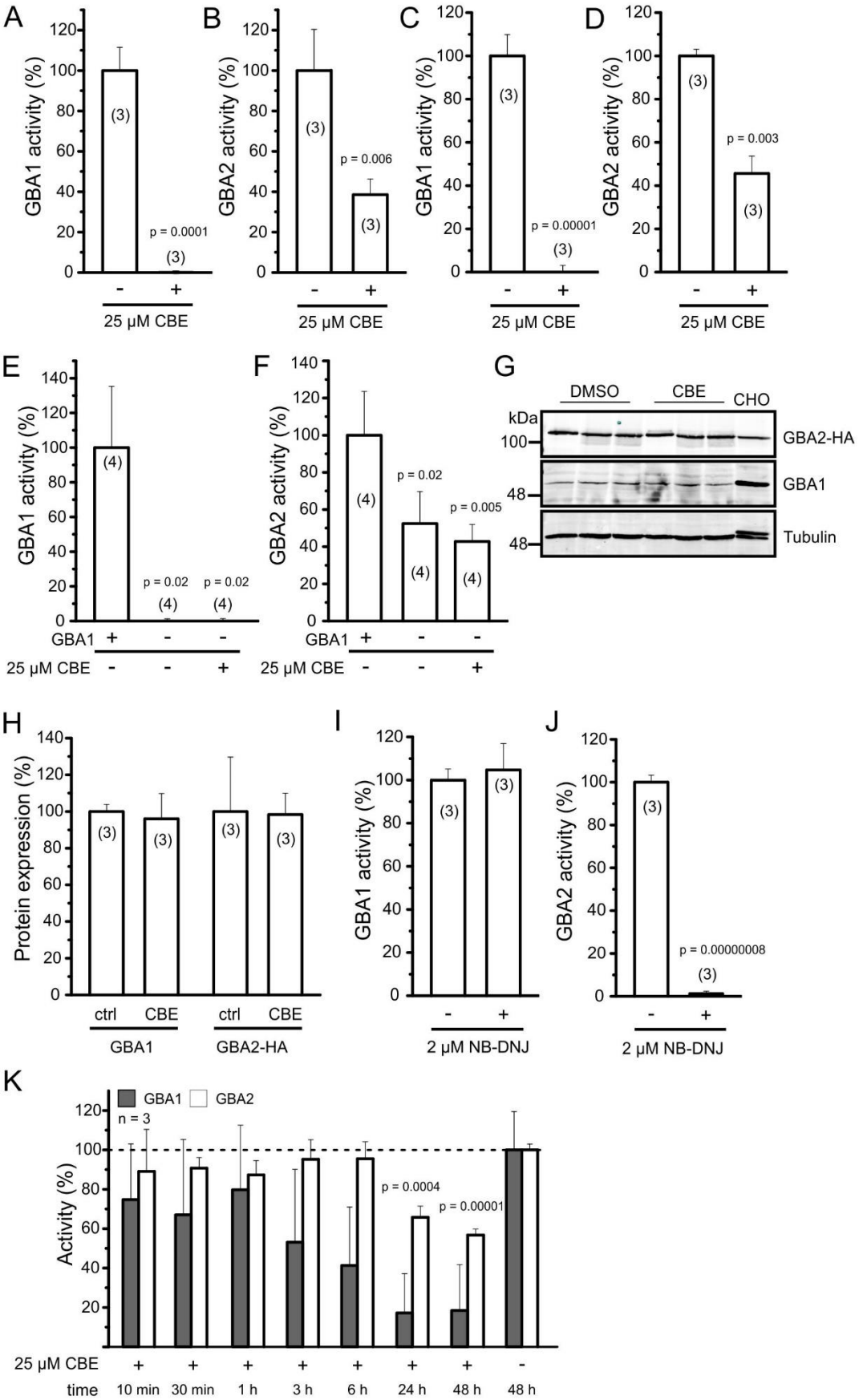

Figure 3

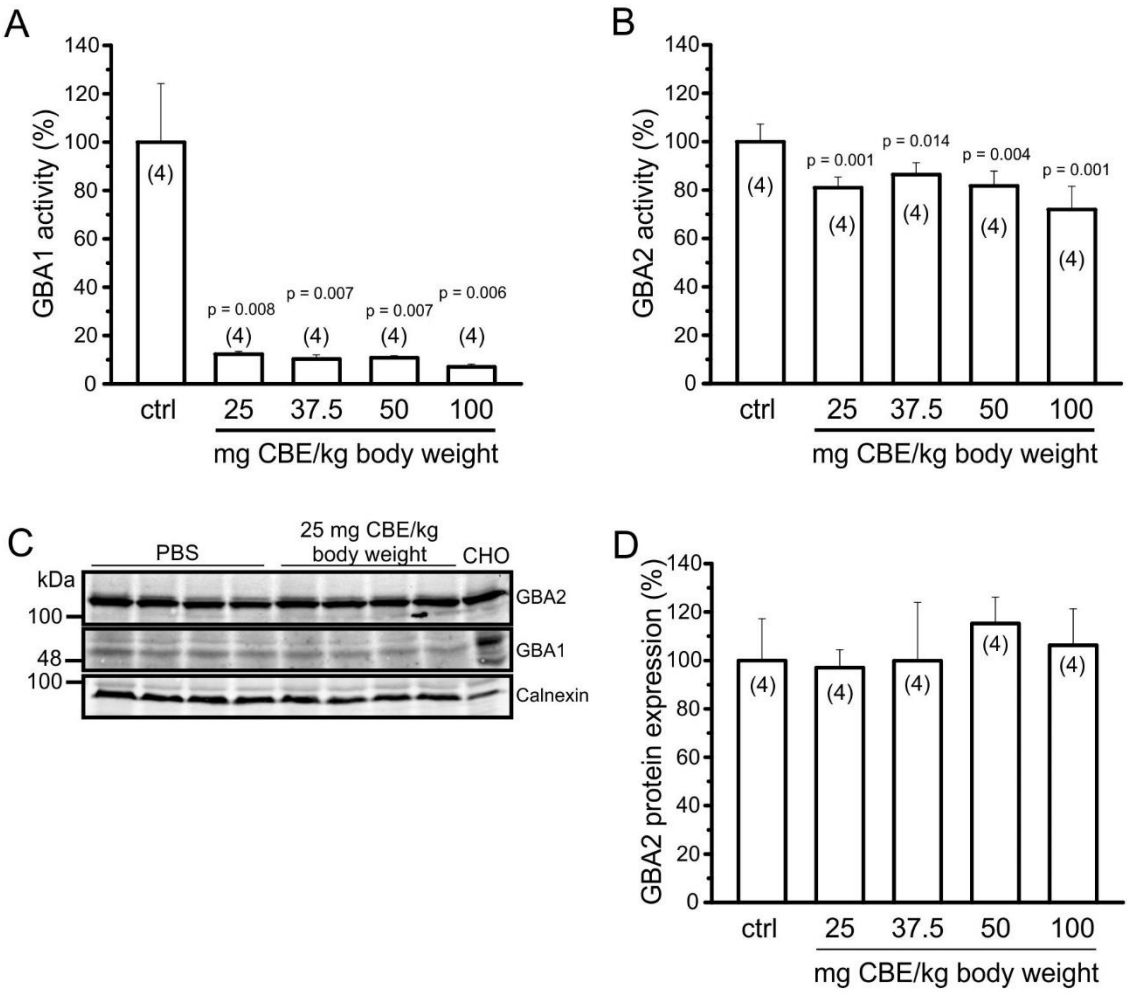

Figure 4

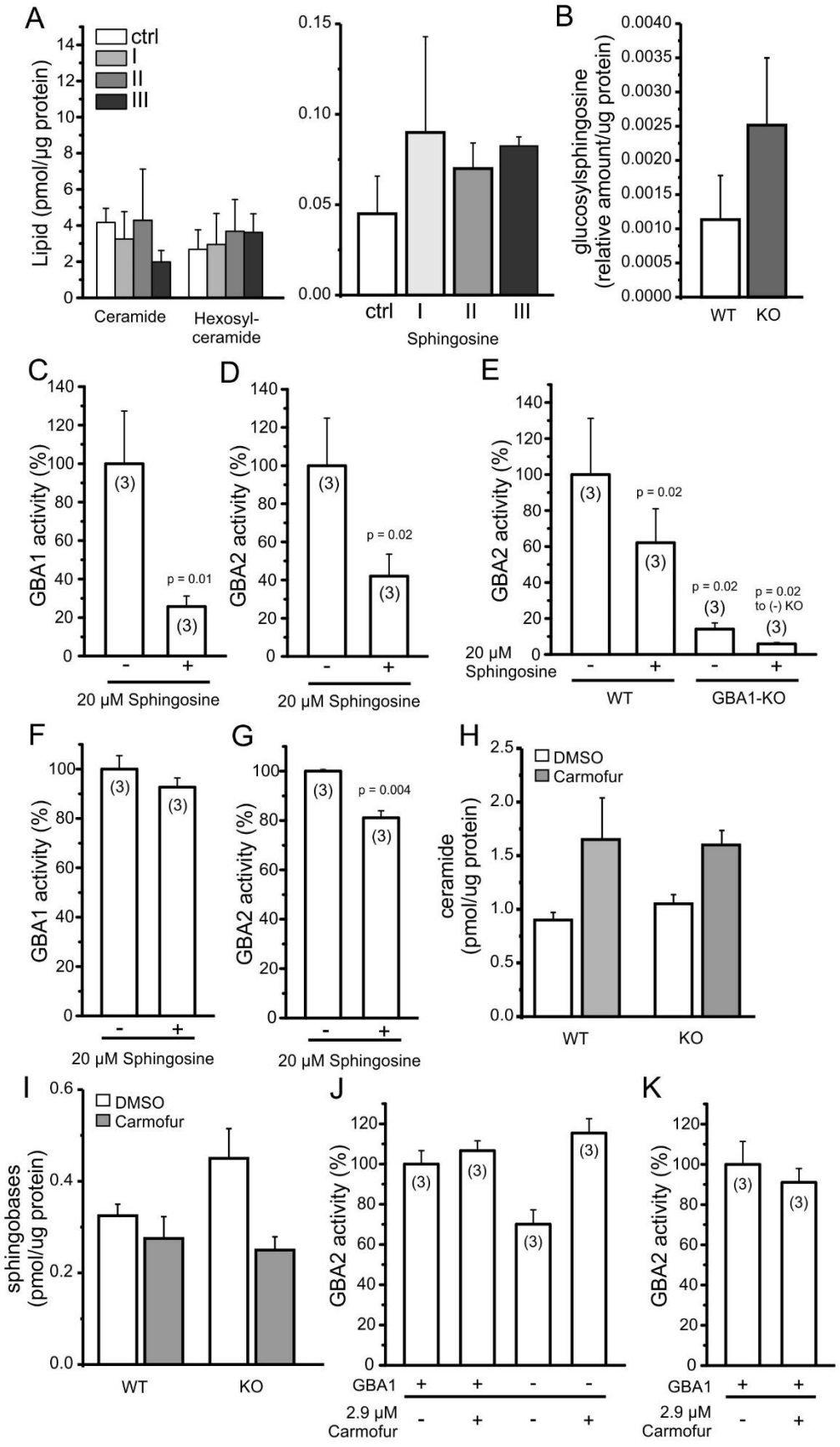

Figure 5

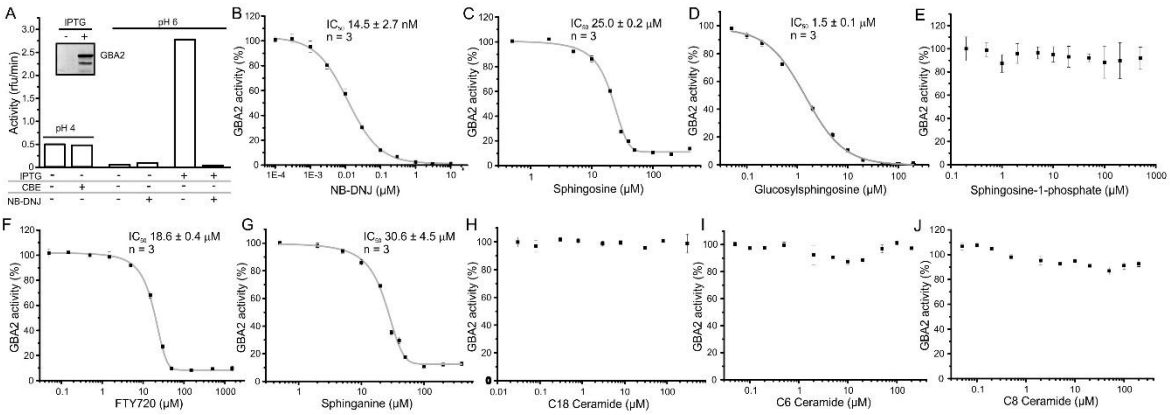

Figure 6

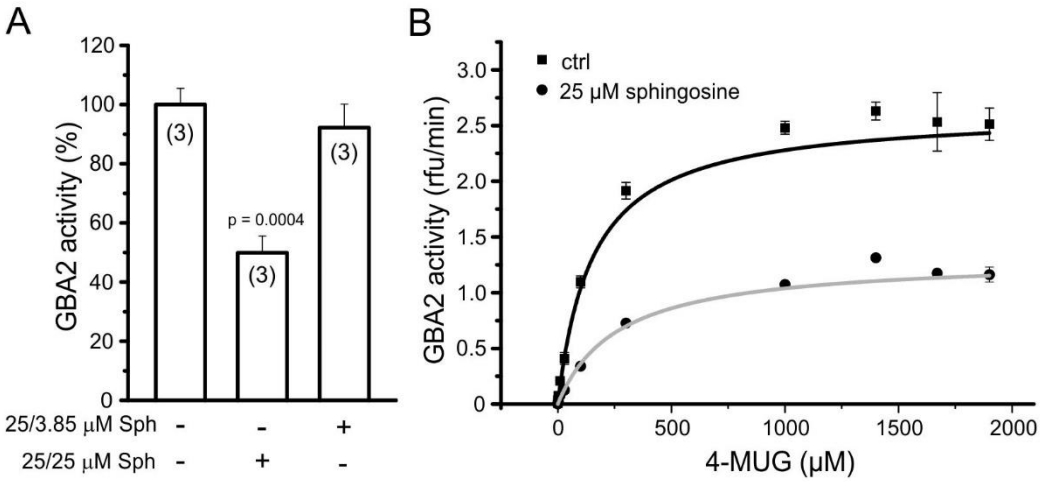

Identification of a feedback loop involving beta-glucosidase 2 and its product sphingosine sheds light on the molecular mechanisms in Gaucher disease

Sophie Schonauer, Heinz G. Körschen, Anke Penno, Andreas Rennhack, Bernadette Breiden, Konrad Sandhoff, Katharina Gutbrod, Peter Dörmann, Diana N. Raju, Per Haberkant, Mathias J. Gerl, Britta Brügger, Hila Zigdon, Ayelet Vardi, Anthony H. Futerman, Christoph Thiele and Dagmar Wachten

J. Biol. Chem. published online March 3, 2017
